ORGANOMETALLICS

pubs.acs.org/Organometallics

Article

Carbon−Carbon Bond Coupling of Vinyl Molecules with an Allenyl Ligand at a Diruthenium Complex

Giulio Bresciani, Stefano Zacchini, Guido Pampaloni, and Fabio Marchetti*

Cite This: *Organometallics* 2022, 41, 1006−1014

Read Online

ACCESS | Metrics & More | Article Recommendations | Supporting Information

ABSTRACT: The room-temperature reactions of the diruthenium μ-allenyl complex $[Ru_2Cp_2(CO)_2(NCMe)\{\mu\text{-}\eta^1{:}\eta^2\text{-}CH{=}C{=}CMe_2\}]BF_4$, **3-NCMe**, with a series of alkenes, $RCH{=}CH_2$, afforded the complexes $[Ru_2Cp_2(CO)_2\{\mu\text{-}\eta^3{:}\eta^2\text{-}CH(R)CHC(Me)C(Me)CH_2\}]BF_4$ (R=Ph, **4**; 4-C_6H_4Me, **5**; Me, **6**; ^{n}Bu, **7**; CO_2Me, **8**; and H, **9**), containing an uncommon pentacarbon alkenyl-allyl ligand. Cross experiments with deuterated reagents, i.e., $[Ru_2Cp_2(CO)_2(NCMe)\{\mu\text{-}\eta^1{:}\eta^2\text{-}CD{=}C{=}CMe_2\}]BF_4$ (**3b-NCMe**) and $CD_2{=}CD(C_6H_5)$ (styrene-d_3), revealed that the formation of **4**−**9** is initiated by an attack of the alkene to the central carbon of the allenyl moiety, triggering two distinct C−H activation processes. Compounds **4**−**9** were characterized by analytical and spectroscopic methods and by single-crystal X-ray diffraction in the cases of **4**, **7**, and **8**. Reported here is the clean coupling on a metallic scaffold between two C_2 and C_3 functions invoked in Fischer−Tropsch mechanistic models.

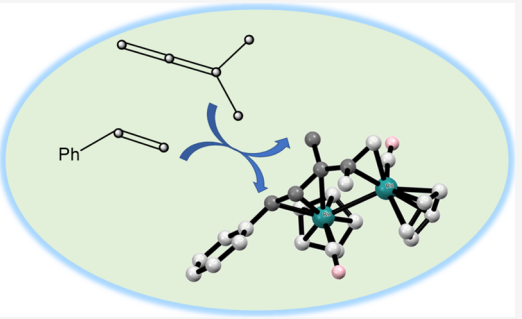

INTRODUCTION

The Fischer−Tropsch synthesis has been established to be a strategic industrial reaction converting carbon monoxide and dihydrogen into useful hydrocarbons with variable chain lengths, in search for alternatives to petroleum.[1] This process is viable on cobalt, iron, and ruthenium surfaces, and among different mechanistic proposals, a plausible pathway has emerged consisting in the preliminary CO deoxygenation to surface carbide, which is then hydrogenated to give {CH}, {CH_2}, and {CH_3} units.[2] One or more of these C_1 species combine together to form an initiating group that, in turn, undergoes sequential coupling with {CH_2} to grow homologous linear chains. In principle, the full elucidation of the mechanistic details is crucial to providing catalyst improvement aimed to optimize the selectivity of the reaction;[3] therefore studies in this regard have aroused a huge interest.[4] Maitlis and co-workers gained useful information by investigating the heterogeneous reaction of CO with H_2 over rhodium/ceria/silica catalysts in the presence of a range of alkenyl probe molecules, and they detected the C_2 probes as incorporated into the hydrocarbon products (no C_2 to C_1 cleavage occurred).[5] As simplified models of the catalyst surface, dinuclear metal complexes with bridging unsaturated hydrocarbyl ligands have been intensively investigated for their reactivity since the last century, with a particular focus on individual C−C coupling events.[6] More specifically, Casey et al. described the feasible interconversion of {CH}, {CH_2}, and {CH_3} bridging ligands on the $[Fe_2Cp_2(CO)_3]$ core,[7] and also the assembly of small unsaturated C_2 and C_1 fragments.[8] Later on, the work by Knox et al. on analogous diruthenium complexes highlighted the straightforward formation of C_2 to C_4 bridging ligands from selective C−C coupling reactions involving alkylidene[9] and alkenyl precursors.[10] Very recently, Matsuzaka and co-workers used a convenient diruthenium bis-pentamethylcyclopentadienide platform to elegantly show that the construction of a C_6 chain proceeds via stepwise addition of {CH_2} blocks to the growing alkenyl function.[11] An allenyl fragment was found to form along this sequence, and the successive chain elongation required H_2 hydrogenation of such C_3 group to go further. The hypothesis that intermediate {C=C=C} species may be implicated in the Fischer−Tropsch mechanism seems reasonable also based on their formation within relevant diiron,[12] dimolybdenum,[13] diruthenium,[14] and diiridium model systems.[15]

Despite the possible key roles played by alkenyl and allenyl functions during the Fischer-−Tropsch synthesis and the numerous related studies on model bimetallic complexes, to the best of our knowledge, their direct coupling has never been reported. We moved to explore a chance for this reaction, and thus we selected a diruthenium carbonyl cyclopentadienyl complex bearing a 3,3-dimethyl-allenyl ligand coordinated in the $\{\mu\text{-}\eta^1{:}\eta^2\}$ fashion.[16] Our choice was suggested by the former evidence that such kind of bridging coordination, in dimetal complexes, favors the activation of the allenyl toward a

Received: February 2, 2022
Published: April 6, 2022

Scheme 1. Allenyl-Alkene Coupling Reaction in a Diruthenium Complex via Preliminary CO-Acetonitrile Replacement

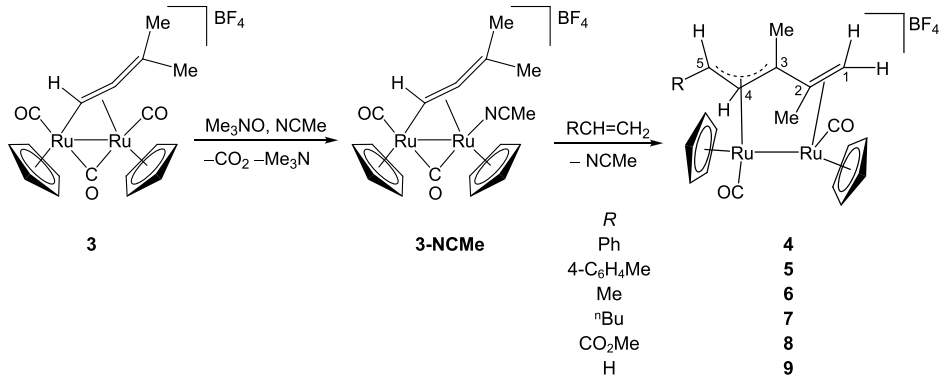

3 3-NCMe

R	
Ph	4
4-C_6H_4Me	5
Me	6
^{n}Bu	7
CO_2Me	8
H	9

range of addition reactions.[17−19] Here, we describe the straightforward alkenylation of the allenyl ligand by a range of vinyl molecules and ethylene.

RESULTS AND DISCUSSION

The diruthenium complex $[Ru_2Cp_2(CO)_3\{\mu\text{-}\eta^1\text{:}\eta^2\text{-}CH{=}C{=}CMe_2\}]BF_4$, **3**, was synthesized from commercial $[Ru_2Cp_2(CO)_4]$ using an optimized literature procedure (see the Supporting Information for details).[18−20] Then, carbonyl displacement was achieved in the presence of acetonitrile using the TMNO strategy;[21] the freshly prepared nitrile adduct $[Ru_2Cp_2(CO)_2(NCMe)\{\mu\text{-}\eta^1\text{:}\eta^2\text{-}CH{=}C{=}CMe_2\}]BF_4$, **3-NCMe**, was allowed to react with monosubstituted alkenes in dichloromethane at room temperature leading to compounds **4**−**8**, which were isolated as microcrystalline solids in 73−89% yields and fully characterized (Scheme 1). The reaction with ethylene affording **9** was accompanied by the formation of a side product; therefore, **9** was characterized in solution only.

The structures of **4**, **7**, and **8** were elucidated by single-=crystal X-ray diffraction. Views of the structures are shown in Figures 1−3 with relevant bond lengths and angles in Table 1.

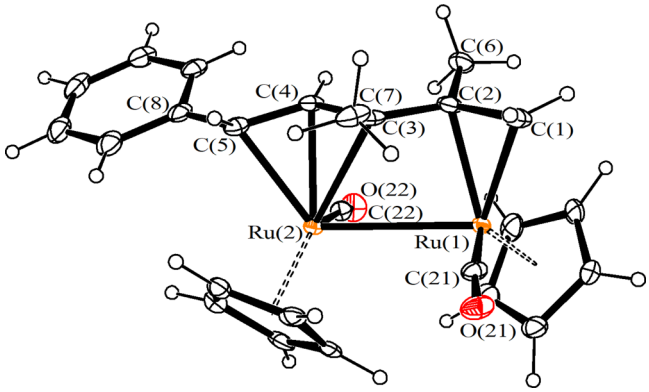

Figure 1. View of the molecular structure of the cation of **4**. Displacement ellipsoids are at the 30% probability level.

The cationic complexes **4**, **7**, and **8** display very similar structures composed of a *trans*-$\{Ru_2Cp_2(CO)_2\}$ core bonded to a $\{\mu\text{-}\eta^2\text{-}\eta^3\text{-}H_2C{=}C(Me){-}C(Me)\cdots C(H)\cdots C(H)(R)\}$ bridging ligand. The Ru−Ru distances [2.9514(10), 2.9718(3), and 2.9767(7) Å for **4**, **7**, and **8**, respectively] are sensibly elongated compared to other diruthenium complexes containing the $\{Ru_2Cp_2(CO)_2\}$ core[22] but in keeping with

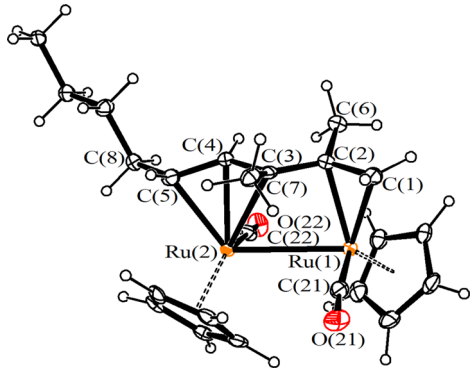

Figure 2. View of the molecular structure of the cation of **7**. Displacement ellipsoids are at the 30% probability level.

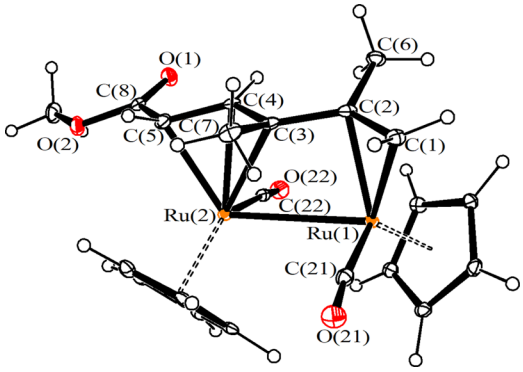

Figure 3. View of the molecular structure of the cation of **8**. Displacement ellipsoids are at the 30% probability level.

Ru−Ru bonding contacts not supported by μ-CO ligands as found in dinuclear complexes and polymetallic clusters.[23] The reported covalent radius of Ru is 1.46 Å,[24] which corresponds to a Ru−Ru bonding distance of 2.92 Å. Here, the observed elongation might be attributed to the steric requirement of the open-chain pentacarbon ligand.

The $\{H_2C{=}C(Me){-}C(Me)\cdots C(H)\cdots C(H)(R)\}$ ligand is η^2 bonded to Ru(1) *via* C(1) and C(2), and η^3 coordinated to Ru(2) through C(3), C(4), and C(5). The Ru(1)···C(3) contact [2.758(6), 2.746(5), and 2.710(3) Å for **4**, **7**, and **8**, respectively] is essentially non-bonding. The C(1)-C(2) [1.417(9), 1.408(8), and 1.417(4) Å for **4**, **7**, and **8**, respectively], C(3)-C(4) [1.428(9), 1.417(8), and 1.422(4) Å], and C(4)-C(5) bonds [1.391(9), 1.386(8), and 1.412(4) Å] display a marked π-character, in agreement with an alkene

https://doi.org/10.1021/acs.organomet.2c00060
Organometallics 2022, 41, 1006−1014

Table 1. Selected Bond Lengths (Å) and Angles (°) for 4, 7, and 8

complexes	4	7	8
Ru(1)-Ru(2)	2.9767(7)	2.9514(10)	2.9718(3)
Ru(1)-Cp_{av}	2.232(16)	2.221(13)	2.232(7)
Ru(2)-Cp_{av}	2.248(15)	2.238(11)	2.246(7)
Ru(1)-C(1)	2.200(7)	2.185(5)	2.204(2)
Ru(1)-C(2)	2.191(6)	2.170(5)	2.188(2)
Ru(1)···C(3)	2.758(6)	2.746(5)	2.710(3)
Ru(2)-C(3)	2.375(6)	2.377(5)	2.431(3)
Ru(2)-C(4)	2.194(6)	2.187(5)	2.189(2)
Ru(2)-C(5)	2.246(6)	2.212(5)	2.182(3)
Ru(1)-C(21)	1.860(7)	1.860(6)	1.863(3)
Ru(2)-C(22)	1.844(6)	1.852(6)	1.874(3)
C(1)-C(2)	1.417(9)	1.408(8)	1.417(4)
C(2)-C(3)	1.454(10)	1.427(8)	1.460(4)
C(3)-C(4)	1.428(9)	1.417(8)	1.422(4)
C(4)-C(5)	1.391(9)	1.386(8)	1.412(4)
C(2)-C(6)	1.523(10)	1.525(8)	1.517(4)
C(3)-C(7)	1.522(10)	1.526(8)	1.521(4)
C(5)-C(8)	1.487(9)	1.472(8)	1.486(4)
C(21)-O(21)	1.141(8)	1.135(7)	1.147(3)
C(22)-O(22)	1.149(8)	1.141(7)	1.139(3)
C(1)-C(2)-C(3)	120.2(7)	121.2(5)	120.1(2)
C(2)-C(3)-C(4)	118.2(6)	119.2(5)	117.1(2)
C(3)-C(4)-C(5)	123.9(6)	126.6(5)	123.6(2)
C(4)-C(5)-C(8)	124.4(6)	122.5(5)	117.8(2)
C(1)-C(2)-C(6)	118.3(7)	118.5(5)	118.4(2)
C(3)-C(2)-C(6)	120.2(6)	118.8(5)	120.2(2)
C(2)-C(3)-C(7)	118.6(6)	118.5(5)	118.6(2)
C(4)-C(3)-C(7)	118.9(6)	118.6(5)	120.6(2)
sum at C(2)	358.7(12)	358.5(9)	358.7(3)
sum at C(3)	355.7(10)	356.3(9)	356.3(3)
Ru(1)-C(21)-O(21)	172.3(6)	173.8(5)	174.0(2)
Ru(2)-C(22)-O(22)	173.3(6)	176.0(5)	171.6(2)
mean deviation from the C(1), C(2), C(3), C(4), C(5), C(6), C(7), and C(8) least-squares planes	0.1650	0.1781	0.1935

and allyl nature for C(1)-C(2) and C(3)-C(4)-C(5), respectively. In contrast, the C(2)-C(3) length [1.454(10), 1.427(8), and 1.460(4) Å for **4**, **7**, and **8**, respectively] is significantly longer and only slightly shorter than C(5)-C(8) [1.487(9), 1.472(8), and 1.486(4) Å]. It is noteworthy that the shortest C(2)-C(3) bond is observed in **7** [1.427(8) Å], displaying an sp^3 hybridization of the C(8) substituent bonded to C(5), whereas C(8) is sp^2 hybridized in **4** and **8**.

The IR and NMR spectra of **4**−**9** are in accordance with the main X-ray features shown by **4**, **7**, and **8**. Thus, the IR spectra of **4**−**7** (in CH_2Cl_2 solution) display two bands related to the terminal carbonyl ligands at ca. 1990 (symmetric stretching) and 1960 cm^{-1} (asymmetric stretching). Due to the decreasing electron donor property of R (decreasing Ru to CO back-donation), the carbonyl absorptions occur at 1998 and 1965 cm^{-1} in **9** (R═H) and at 2024 and 1974 cm^{-1} in **8** (R═CO_2Me). The ^1H and ^{13}C NMR spectra (CD_2Cl_2 solution) of **4**−**9** consist of a single set of resonances. In the ^1H NMR spectra, the Cp ligands are seen at ca. 5.6 and 5.4 ppm, in accordance with the trans geometry,[9b] which has also been recognized in the solid-state structures; since **3** prevalently exists as a *cis* isomer, the formation of **4**−**9** takes place with *cis* to *trans* rearrangement. The allylic C^5−H and C^4−H hydrogens resonate within the ranges 5.70−4.44 and 4.24−3.34 ppm,[25] respectively, and the C^1H_2 group gives rise to two distinct signals at significantly different chemical shifts (e.g., at 4.08 and 2.64 ppm in the case of **4**). Salient ^{13}C NMR features are provided by the two terminal carbonyl ligands (197−204 ppm) and the five carbons directly involved in metal coordination [e.g., in the case of **4**: δ/ppm = 39.2 (C^1), 70.9 (C^2), 73.7 (C^3), 76.0 (C^4), and 67.8 (C^5)]. This set of data supports the best description of the pentacarbon ligand as alkenyl-allyl.[25b,26,27]

With the aim of elucidating the allenyl-alkene coupling, we repeated the reaction leading to **4** by using deuterated reagents. First, we prepared the deuterated analogue of **3** (complex **3b**, see the Experimental Sectio for details). The subsequent reaction of the nitrile adduct **3b-NCMe** with styrene revealed that alkenyl addition occurs at the central

Scheme 2. Cross Reactions with Deuterated Reagents: (A) Reaction of the Allenyl-d_1 Complex (3b-NCMe) with Styrene, (B) Reaction of the Allenyl Complex (3-NCMe) with Styrene-d_3; Inset: Carbon Atom Numbering for the Final η^5-ligand (see also Scheme 1)

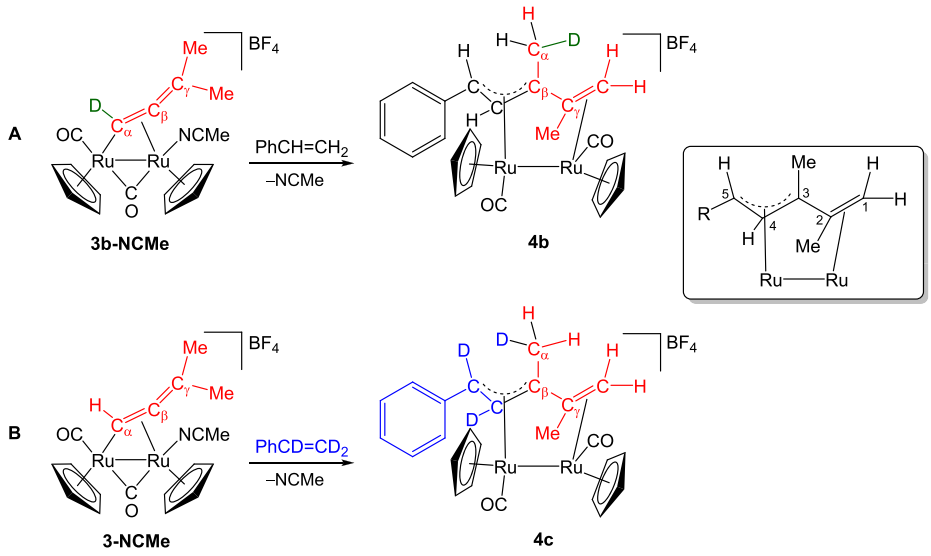

https://doi.org/10.1021/acs.organomet.2c00060
Organometallics 2022, 41, 1006−1014

Scheme 3. Proposed Steps for Allenyl-Alkene Coupling, Cationic Charge and Counteranion have been Omitted for Clarity

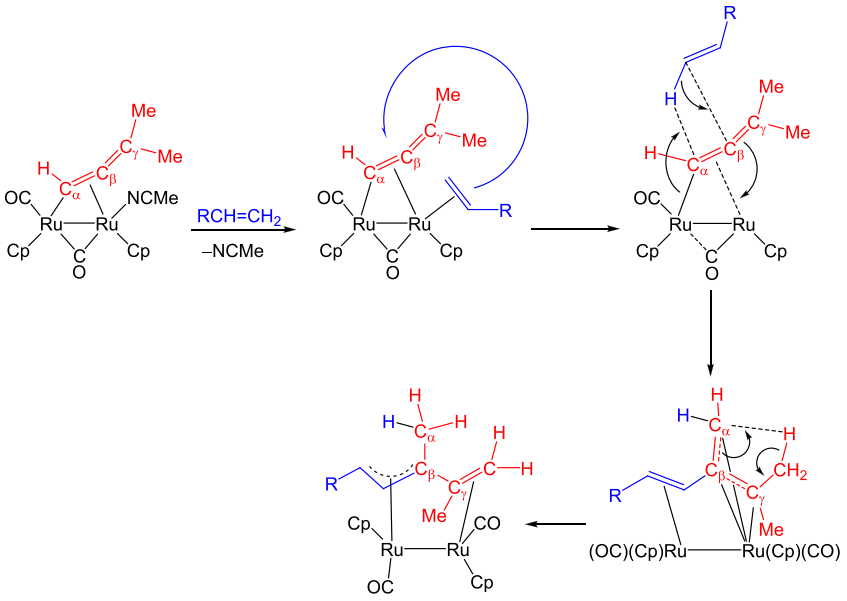

carbon (C_β) of the allenyl moiety (Scheme 2A). The resulting complex **4b** was characterized by ^{1}H and ^{2}H NMR spectroscopies, which agreed in showing the C_α allenyl carbon converted into a methyl group, i.e., C^3-Me in the final ligand. As C^3-Me resonates at 0.72 ppm in the ^{1}H NMR spectrum of **4**, one multiplet was observed at 0.72 ppm in the ^{1}H and ^{2}H NMR spectra of **4b**. On the other side, the treatment of **3-NCMe** with styrene-d_3 allowed one to locate the hydrogen atom arising from alkene activation (Scheme 2B). As a matter of fact, the ^{2}H NMR spectrum of **4c** exhibited two signals at 5.75 and 4.27 ppm, accounting for two deuterium nuclei in the allyl moiety and one signal at 0.72 ppm, resembling that recognized in the ^{2}H spectrum of **4b**. The merged information provided by the deuterium-labeled experiments indicate that one C_γ-methyl belonging to the starting allenyl ligand undergoes loss of one hydrogen, migrating to C_α.

Combined, the NMR study hints at the following sequence of reaction stages (Scheme 3). First, η^2-alkene coordination to the ruthenium is enabled by substitution of the labile acetonitrile ligand of **3-NCMe**. This is a needed preliminary step for the subsequent alkene interaction with the bridging allenyl, in alignment with that previously proposed for a number of coupling reactions between various hydrocarbyl ligands, bridging coordination in dimetal complexes, and alkenes[28] or alkynes.[9b,29] Indeed, complex **3** was unreactive toward styrene even under high-temperature conditions. Accordingly, it was demonstrated that hydride addition to a complex closely related to **3-NCMe** proceeds with the initial formation of a metal-hydride species followed by hydride migration to the allenyl C_α-carbon.[19] In the present case, the alkene should migrate from the terminal coordination site to attack the C_β[30] with its non-substituted carbon; although mechanistic details cannot be provided at the present level, this migration appears to be accompanied by Csp^2–H activation and consequent transfer of the hydrogen to the adjacent C_α. Note that in **4**–**9**, ruthenium centers maintain the +II oxidation state as in **1**; therefore, oxidative steps appear unlikely. Attempts to extend the reaction scope to disubstituted alkenes, both internal [e.g., *cis*- and *trans*-(CO_2Me)CH=CH(CO_2Me), cyclohexene] and terminal ones [e.g., CH_2=C(*Me*)CO_2Me, CH_2=C(*Me*)Ph], did not result in any reaction, thus confirming the importance of steric factors in driving the C–C coupling. Finally, an intramolecular hydrogen migration from one C_γ-methyl to C_α finalizes the formation of the $\{\mu\text{-}\eta^3\text{:}\eta^2\}$ ligand. During this overall pathway, the mutual geometry of the Cp rings (*cis* or *trans*) and the coordination of the CO ligands (terminal or bridging) are expected to interconvert according to the Adams–Cotton mechanism, which is pivoted on rotation around the metal–metal axis and is responsible for *cis-trans* isomerizations in related diruthenium and diiron complexes.[31]

CONCLUSIONS

Diruthenium complexes with bridging unsaturated hydrocarbyl ligands constitute ideal platforms to model possible key steps involved in the Fischer–Tropsch heterogeneous reaction, which still arouses a huge interest for its strategic implications. A great amount of work has been done in this field, evidencing that the C–C bond coupling of small molecular blocks is feasible under mild conditions. It is generally accepted that alkenyl groups play a fundamental role in the growing chain process; instead, the intermediate formation of allenyl moieties has been supported even by very recent findings, but their direct engagement in the FT remains obscure. Here, we demonstrate that an allenyl ligand, bridging coordinated in a diruthenium carbonyl cyclopentadienyl complex, undergoes facile C–C coupling with a variety of mono-substituted alkenes and ethylene once a metal coordination vacancy is generated. This rare reaction proceeds with alkene attack to the central carbon of the allenyl chain followed by multiple hydrogen migration providing access to an uncommon example of a pentacarbon allyl-alkenyl ligand. Our result contributes to the understanding of the multifaceted Fischer–Tropsch process, disclosing the possibility of a single reaction event (i.e., allenyl-alkene coupling) that has received scarce attention heretofore. This may represent a possible pathway for the formation of minor branched hydrocarbons in the FT products, at variance with the predominant formation of linear hydrocarbon chains.

https://doi.org/10.1021/acs.organomet.2c00060
Organometallics 2022, 41, 1006–1014

EXPERIMENTAL SECTION

Materials and Methods. Reactants and solvents were purchased from Alfa Aesar, Merck, Strem, or TCI Chemicals and were of the highest purity available. Complexes **1**[20] and **3**[18,19] were prepared by a slight modification of the literature procedure (see the Supporting Information). Reactions were conducted under a N_2 atmosphere using standard Schlenk techniques. Products were stored in air once isolated. Dichloromethane and diethyl ether were dried using the solvent purification system mBraun MB SPS5, while acetonitrile was distilled from CaH_2. The IR spectra of solutions were recorded using a CaF_2 liquid transmission cell (2300−1500 cm^{-1}) on a Perkin Elmer Spectrum 100 FT-IR spectrometer. The IR spectra were processed with Spectragryph software.[32,33] The ^1H, ^{13}C, and ^2H NMR spectra were recorded at 298 K on a Jeol JNM-ECZ500R instrument equipped with a Royal HFX Broadband probe. Chemical shifts (expressed in parts per million) are referenced to the residual solvent peaks.[34] The NMR spectra were assigned with the assistance of ^1H-^{13}C (*gs*-HSQC and *gs*-HMBC) correlation experiments.[35] Elemental analyses were performed on a Vario MICRO cube instrument (Elementar).

Synthesis of Complexes 4−9. *General Procedure.* Complex **3** (*ca.* 0.180 mmol) was dissolved in CH_2Cl_2 (25 mL) and treated with 1.0 equiv Me_3NO in MeCN solution (0.10 M). The mixture was stirred for 15 min; then, the formation of the acetonitrile adduct **3-NCMe** was checked by IR spectroscopy [IR (CH_2Cl_2): $\tilde{\nu}/cm^{-1}$ = 2003s (CO), 1853br-m (μ-CO)].[19] Volatiles were removed under vacuum to give a brown residue, which was dissolved in CH_2Cl_2 (25 mL), and the selected alkene (5−10 equiv) was added to this solution. The resulting mixture was stirred overnight at room temperature; then, the solvent was removed under reduced pressure. The obtained residue was washed with Et_2O (3 × 15 mL) and dried under vacuum.

$[Ru_2Cp_2(CO)_2\{\mu\text{-}\eta^3\text{:}\eta^2\text{-}CH(Ph)CHC(Me)C(Me)CH_2\}]BF_4$, **4** (*Figure 4*). From **3** (106 mg, 0.186 mmol), Me_3NO (14.0 mg, 0.186 mmol), and styrene (0.20 mL, 1.7 mmol). Orange solid, yield 103 mg (86%). Anal. calcd. for $C_{25}H_{25}BF_4O_2Ru_2$: C, 46.45; H, 3.90. Found: C, 46.49; H, 3.98. IR (CH_2Cl_2): $\tilde{\nu}/cm^{-1}$ = 2000w-sh (CO), 1962vs (CO). ^1H NMR (CD_2Cl_2): δ/ppm = 7.59−7.40 (m, 5 H, Ph); 5.70 (d, $^3J_{HH}$ = 11.7 Hz, 1 H, C^5H); 5.51, 5.44 (s, 10 H, Cp); 4.24 (d, $^3J_{HH}$ = 11.7 Hz, 1 H, C^4H); 4.08 (d, $^2J_{HH}$ = 2.3 Hz, 1 H, C^1H); 2.64 (d, $^2J_{HH}$ = 2.0 Hz, 1 H, C^1H); 1.80 (s, 3 H, C^2Me); 0.72 (s, 3 H, C^3Me). $^{13}C\{^1H\}$ NMR (CD_2Cl_2): δ/ppm = 203.9, 200.5 (CO); 138.8 (ipso-Ph); 130.0, 129.6, 127.2 (Ph); 91.7, 88.7 (Cp); 76.0 (C^4); 73.7 (C^3); 70.9 (C^2); 67.8 (C^5); 39.2 (C^1); 25.2 (C^2Me); 18.9 (C^3Me). Crystals suitable for X-ray analysis were collected by slow diffusion of diethyl ether into a dichloromethane solution of **4** at room temperature.

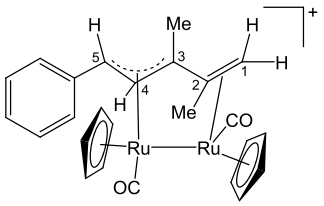

Figure 4. Structure of the cation of **4**.

$[Ru_2Cp_2(CO)_2\{\mu\text{-}\eta^3\text{:}\eta^2\text{-}CH(4\text{-}MeC_6H_4)CHC(Me)C(Me)CH_2\}]BF_4$, **5** (*Figure 5*). From **3** (100 mg, 0.175 mmol), Me_3NO (13.2 mg, 0.176 mmol), and 4-methylstyrene (0.20 mL, 1.52 mmol). Yellow solid, yield 84 mg (73%). Anal. calcd. for $C_{26}H_{27}BF_4O_2Ru_2$: C, 47.28; H, 4.12. Found: C, 47.35; H, 4.24. IR (CH_2Cl_2): $\tilde{\nu}/cm^{-1}$ = 1995w-sh (CO), 1962vs (CO). ^1H NMR (CD_2Cl_2): δ/ppm = 7.48−7.27 (m, 4 H, C_6H_4); 5.70 (d, $^3J_{HH}$ = 11.7 Hz, 1 H, C^5H); 5.49, 5.42 (s, 10 H, Cp); 4.23 (d, $^3J_{HH}$ = 11.7 Hz, 1 H, C^4H); 4.06 (d, $^2J_{HH}$ = 2.3 Hz, 1 H, C^1H); 2.65 (d, $^2J_{HH}$ = 2.0 Hz, 1 H, C^1H); 2.40 (s, 3 H, C_6H_4Me); 1.80 (s, 3H, C^2Me); 0.72 (s, 3H, C^3Me). $^{13}C\{^1H\}$ NMR (CD_2Cl_2): δ/ppm = 204.1, 200.8 (CO); 140.1, 135.9, 130.7, 127.2 (C_6H_4); 91.7, 88.7 (Cp); 75.5 (C^4); 73.5 (C^3); 70.8 (C^2); 68.8 (C^5); 39.1 (C^1); 25.2 (C^2Me); 21.5 (C_6H_4Me); 18.9 (C^3Me).

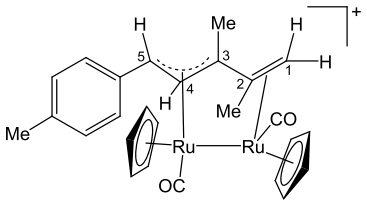

Figure 5. Structure of the cation of **5**.

$[Ru_2Cp_2(CO)_2\{\mu\text{-}\eta^3\text{:}\eta^2\text{-}CH(Me)CHC(Me)C(Me)CH_2\}]BF_4$, **6** (*Figure 6*). From **3** (103 mg, 0.181 mmol), Me_3NO (13.6 mg, 0.181 mmol), and excess of propene bubbled into the reaction solution. Pale-brown solid, yield 94 mg (89%). Anal. calcd. for $C_{20}H_{23}BF_4O_2Ru_2$: C, 41.11; H, 3.97. Found: C, 41.15; H, 3.94. IR (CH_2Cl_2): $\tilde{\nu}/cm^{-1}$ = 1992w (CO), 1963vs (CO). ^1H NMR (CD_2Cl_2): δ/ppm = 5.62, 5.41 (s, 10 H, Cp); 4.87 (m, 1 H, C^5H); 4.08 (d, $^2J_{HH}$ = 2.3 Hz, 1 H, C^1H); 3.42 (d, $^3J_{HH}$ = 11.4 Hz, 1 H, C^4H); 2.57 (d, $^2J_{HH}$ = 2.3 Hz, 1 H, C^1H); 2.26 (d, $^3J_{HH}$ = 6.0 Hz, 3 H, C^5Me); 1.67 (s, 3 H, C^2Me); 0.54 (s, 3 H, C^3Me). $^{13}C\{^1H\}$ NMR (CD_2Cl_2): δ/ppm = 204.1, 200.4 (CO); 90.9, 88.6 (Cp); 80.5 (C^4); 73.3 (C^3); 72.1 (C^2); 65.7 (C^5); 39.1 (C^1); 25.0 (C^2Me); 23.2 (C^5Me); 18.8 (C^3Me).

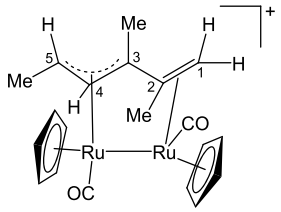

Figure 6. Structure of the cation of **6**.

$[Ru_2Cp_2(CO)_2\{\mu\text{-}\eta^3\text{:}\eta^2\text{-}CH(CH_2CH_2CH_2CH_3)CHC(Me)C(Me)CH_2\}]BF_4$, **7** (*Figure 7*). From **3** (108 mg, 0.189 mmol), Me_3NO (14.2 mg, 0.189 mmol), and 1-hexene (0.16 mL, 1.32 mmol). Brown solid, yield 95 mg (84%). Anal. calcd. for $C_{23}H_{29}BF_4O_2Ru_2$: C, 44.10; H, 4.67. Found: C, 44.15; H, 4.72. IR (CH_2Cl_2): $\tilde{\nu}/cm^{-1}$ = 1992w-sh (CO), 1961vs (CO). ^1H NMR (CD_2Cl_2): δ/ppm = 5.63, 5.42 (s, 10 H, Cp); 4.78 (m, 1 H, C^5H); 4.05 (d, $^2J_{HH}$ = 2.3 Hz, 1 H, C^1H); 3.34 (d, $^3J_{HH}$ = 11.5 Hz, 1 H, C^4H); 2.63, 2.04−1.97 (m, 2 H, C^5CH_2); 2.56 (d, $^2J_{HH}$ = 2.0 Hz, 1 H, C^1H); 1.91−1.81, 1.74−1.68, 1.66 (m, 5 H, $C^5CH_2CH_2$ + C^2Me); 1.59−1.51 (m, 2 H, CH_2CH_3); 1.02 (t, $^3J_{HH}$ = 7.4 Hz, 3 H, CH_2CH_3); 0.54 (s, 3 H, C^3Me). $^{13}C\{^1H\}$ NMR (CD_2Cl_2): δ/ppm = 204.0, 200.4 (CO); 90.5, 88.6 (Cp); 79.7 (C^4); 73.5 (C^3); 72.3 (C^2); 70.5 (C^5); 39.3 (C^1); 38.2 (C^5CH_2); 35.2 ($C^5CH_2CH_2$); 25.1 (C^2Me); 22.9 (CH_2CH_3); 19.0 (C^3Me); 14.0 (CH_2CH_3). Crystals suitable for X-ray analysis were collected by slow diffusion of diethyl ether into a dichloromethane solution of **7** at room temperature.

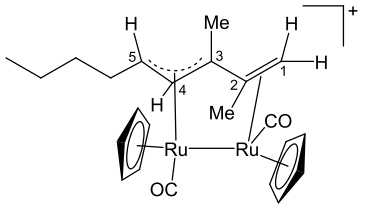

Figure 7. Structure of the cation of **7**.

$[Ru_2Cp_2(CO)_2\{\mu\text{-}\eta^3\text{:}\eta^2\text{-}CH(CO_2Me)CHC(Me)C(Me)CH_2\}]BF_4$, **8** (*Figure 8*). From **3** (100 mg, 0.175 mmol), Me_3NO (13.2 mg, 0.176 mmol), and methyl acrylate (0.10 mL, 1.10 mmol). Red solid, yield 88 mg (80%). Anal. calcd. for $C_{21}H_{23}BF_4O_4Ru_2$: C, 40.14; H, 3.69.

https://doi.org/10.1021/acs.organomet.2c00060
Organometallics 2022, 41, 1006−1014

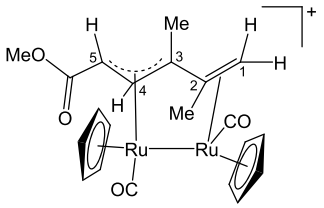

Figure 8. Structure of the cation of **8**.

Found: C, 40.18; H, 3.73. IR (CH_2Cl_2): $\tilde{\nu}/cm^{-1}$ = 2024w (CO), 1974vs (CO), 1726s (COO). ^1H NMR (CD_2Cl_2): δ/ppm = 5.70, 5.49 (s, 10 H, Cp); 4.44 (d, $^3J_{HH}$ = 10.4 Hz, 1 H, C^5H); 4.24 (d, $^2J_{HH}$ = 2.4 Hz, 1 H, C^1H); 4.00 (d, $^3J_{HH}$ = 10.6 Hz, 1 H, C^4H); 3.92 (s, 3 H, OMe); 2.28 (d, $^2J_{HH}$ = 2.3 Hz, 1 H, C^1H); 1.80 (s, 3 H, C^2Me); 0.72 (s, 3 H, C^3Me). $^{13}C\{^1H\}$ NMR (CD_2Cl_2): δ/ppm = 202.7, 197.4 (CO); 172.5 (OCO); 91.0, 89.0 (Cp); 79.7 (C^4); 75.4 (C^3); 75.3 (C^2); 53.2 (OMe); 47.1 (C^5); 41.0 (C^1); 24.7 (C^2Me); 18.9 (C^3Me). Crystals suitable for X-ray analysis were collected by slow diffusion of heptane into a dichloromethane solution of **8** at room temperature.

$[Ru_2Cp_2(CO)_2\{\mu\text{-}\eta^3\text{:}\eta^2\text{-}CH_2CHC(Me)C(Me)CH_2\}]BF_4$, ***9*** (*Figure 9*). From **3** (106 mg, 0.186 mmol), Me_3NO (14.0 mg, 0.186 mmol), and

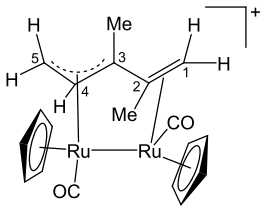

Figure 9. Structure of the cation of **9**.

excess of ethylene bubbled into the reaction solution. Brown solid, yield 100 mg (52% estimated according to ^1H NMR). IR (CH_2Cl_2): $\tilde{\nu}/cm^{-1}$ = 1998w (CO), 1965s (CO). ^1H NMR (acetone-d_6): δ/ppm = 5.54, 5.43 (s, 10 H, Cp); 4.54 (dd, $^3J_{HH}$ = 7.2 Hz, $^2J_{HH}$ = 1.4 Hz, 1 H, C^5H); 4.31 (d, $^2J_{HH}$ = 1.9 Hz, 1 H, C^1H); 4.13 (dd, $^3J_{HH}$ = 12.0 Hz, $^2J_{HH}$ = 1.4 Hz, 1 H, C^5H); 3.72 (dd, $^3J_{HH}$ = 7.3 Hz, 1 H, C^4H); 2.69 (d, $^2J_{HH}$ = 1.9 Hz, 1 H, C^1H); 1.78 (s, 3 H, C^2Me); 0.61 (s, 3 H, C^3Me). $^{13}C\{^1H\}$ NMR (acetone-d_6): δ/ppm = 204.0, 199.3 (CO); 90.1, 88.6 (Cp); 78.3 (C^4); 75.9 (C^2); 74.0 (C^3); 54.8 (C^5); 38.7 (C^1); 24.7 (C^2Me); 16.8 (C^3Me). An inseparable, unidentified by-product (**9′**) was detected in an admixture with **9**. IR (CH_2Cl_2): $\tilde{\nu}/cm^{-1}$ = 1830 (CO). ^1H NMR (acetone-d_6): δ/ppm = 5.98, 5.73 (s, Cp); 3.49, 2.96 (dd); 2.27, 1.43 (s). $^{13}C\{^1H\}$ NMR (acetone-d_6): 226.4, 207.7 (CO); 94.3, 93.2 (Cp); 25.9, 23.9 (Me). **9**/**9′** ratio = 55:45.

Synthesis of 2-Methylbut-3-yn-4-*d*-2-ol-*d* (Figure 10). A 2.5 M hexane solution of butyllithium (9.0 mL, 23 mmol) was added

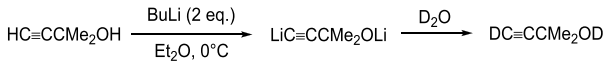

Figure 10. Preparation of 2-methylbut-3-yn-4-*d*-2-ol-*d*.

dropwise to an ice-cooled, stirred solution of 2-methylbut-3-yn-2-ol (1.00 mL, 10.3 mmol) in diethyl ether (40 mL). Then, the ice bath was removed, and the solution was stirred for further 90 min at room temperature. The final mixture was quenched with D_2O (5.0 mL); thus, the organic phase was separated and dried under reduced pressure. Colorless liquid, yield 506 mg (57%). ^1H NMR ($CDCl_3$): δ/ppm = 1.53 (s, 6 H, Me).

Synthesis of $[Ru_2Cp_2(CO)_2(\mu\text{-}CO)\{\mu\text{-}\eta^1\text{:}\eta^2\text{-}CD{=}C{=}C(Me)(Me)\}]BF_4$, 3b (Figure 11). A solution of **1** (60.0 mg, 0.101 mmol) in toluene (20 mL) was treated with 2-methylbut-3-yn-4-*d*-2-ol-*d* (90 mg, 1.04 mmol). The resulting mixture was stirred at reflux temperature for 1 h, during which time the consumption of **1** and the formation of **2b** were checked by IR spectroscopy [IR (CH_2Cl_2): $\tilde{\nu}/cm^{-1}$ = 1978vs (CO), 1803s (μ-CO), 1734br-m (C═O)]. The final solution was allowed to cool to room temperature, and the solvent was removed under reduced pressure at 50 °C. The red solid residue was washed with pentane (2 × 15 mL); then, it was dissolved in CH_2Cl_2 (15 mL), and $HBF_4{\cdot}Et_2O$ (14.0 μL, 0.103 mmol) was added dropwise to this solution. Stirring was maintained for 15 min at room temperature. The final solution was added with D_2O (5 mL) and the mixture was vigorously shaken. The organic phase was separated, and volatiles were removed under reduced pressure. The solid was dissolved in the minimum volume of CH_2Cl_2 (ca. 2 mL), and precipitation with diethyl ether (30 mL) afforded **3b** as a yellow solid, which was washed with diethyl ether (3 × 15 mL) and dried under vacuum. Yield 38 mg, 66%. IR (CH_2Cl_2): $\tilde{\nu}/cm^{-1}$ = 2040vs (CO), 2020 m (CO), 1873 m-w (μ-CO).

Synthesis of $[Ru_2Cp_2(CO)_2\{\mu\text{-}\eta^3\text{:}\eta^2\text{-}CH(Ph)CHC(CH_2D)C(Me)CH_2\}]BF_4$, 4b, from 3b and Styrene (Figure 12). The title compound was obtained by the same procedure as that described for the syntheses of **4**−**8**, from **3b** (46 mg, 0.080 mmol), Me_3NO (6.0 mg, 0.080 mmol), and styrene (0.10 mL, 0.87 mmol). The preliminary formation of the acetonitrile adduct **3b-NCMe** was checked by IR spectroscopy [IR (CH_2Cl_2): $\tilde{\nu}/cm^{-1}$ = 2003s (CO), 1853br-m (μ-CO)]. Brown solid, yield 39 mg (75%). IR (CH_2Cl_2): $\tilde{\nu}/cm^{-1}$ = 1996w-sh (CO), 1963vs (CO). ^1H NMR (CD_2Cl_2): δ/ppm = 7.59−7.57, 7.48−7.42 (m, 5 H, Ph); 5.67 (d, $^3J_{HH}$ = 11.7 Hz, 1 H, C^5H); 5.51, 5.43 (s, 10 H, Cp); 4.24 (d, $^3J_{HH}$ = 11.7 Hz, 1 H, C^4H); 4.08, 2.65 (m, 2 H, C^1H); 1.80 (s, 3 H, C^2Me); 0.72 (m, 2 H, CH_2D). ^2H NMR (CH_2Cl_2): δ/ppm = 0.72 (br, 1 D, CH_2D).

Synthesis of $[Ru_2Cp_2(CO)_2\{\mu\text{-}\eta^3\text{:}\eta^2\text{-}CD(Ph)CDC(CH_2D)C(Me)CH_2\}]BF_4$, 4c, from 3 and Styrene-d_3 (Figure 13). This reaction was conducted using the same procedure as that described for the syntheses of **4**−**8**, from **3** (98.0 mg, 0.172 mmol), Me_3NO (12.9 mg, 0.172 mmol), and styrene-d_3 (0.10 mL, 0.87 mmol). Dark-orange solid, yield 93 mg (83%). IR (CH_2Cl_2): $\tilde{\nu}/cm^{-1}$ = 1993w-sh (CO), 1962vs (CO). ^1H NMR (CD_2Cl_2): δ/ppm = 7.59−7.57, 7.49−7.42 (m, 5 H, Ph); 5.51, 5.43 (s, 10 H, Cp); 4.08 (d, $^2J_{HH}$ = 2.3 Hz, 1 H, C^1H); 2.64 (d, $^2J_{HH}$ = 2.0 Hz, 1 H, C^1H); 1.80 (s, 3 H, C^2Me); 0.72 (m, 2 H, CH_2D). ^2H NMR (CH_2Cl_2): δ/ppm = 5.75 (s, 1 D, C^5D); 4.27 (s, 1 D, C^4D); 0.72 (br, 1 D, CH_2D).

X-ray Crystallography. Crystal data and collection details for **4**, **7**, and **8** are reported in Table 2. Data were recorded on a Bruker APEX II diffractometer equipped with a PHOTON2 detector using Mo−Kα radiation. The structures were solved by direct methods and refined by full-matrix least-squares based on all data using F^2.[36] Hydrogen atoms were fixed at calculated positions and refined using a riding model.[37]

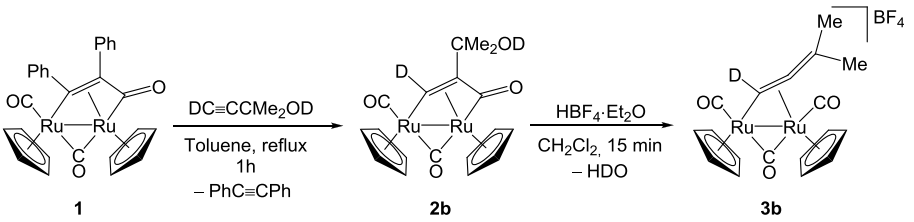

Figure 11. Synthesis of **3b**.

https://doi.org/10.1021/acs.organomet.2c00060
Organometallics 2022, 41, 1006−1014

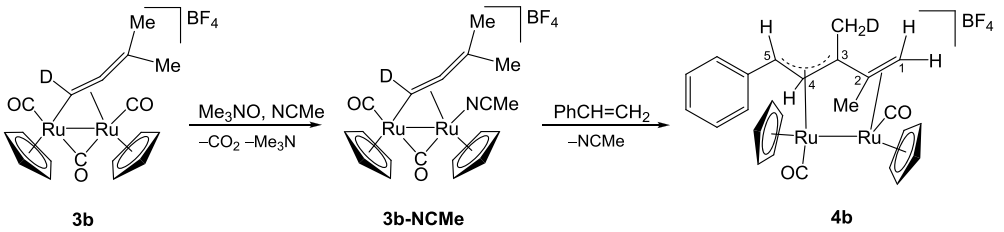

Figure 12. Synthesis of **4b**.

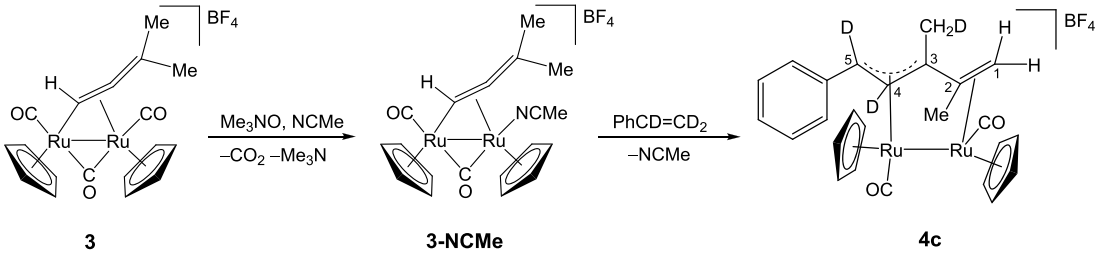

Figure 13. Synthesis of **4c**.

Table 2. Crystal Data and Measurement Details for 4, 7, and 8

parameters	4	7	8
formula	$C_{25}H_{25}BF_4O_2Ru_2$	$C_{23}H_{29}BF_4O_2Ru_2$	$C_{21}H_{23}BF_4O_4Ru_2$
FW	646.40	626.41	628.34
T, K	100(2)	100(2)	100(2)
λ, Å	0.71073	0.71073	0.71073
crystal system	monoclinic	monoclinic	monoclinic
space group	$P2_1/c$	$P2_1/c$	$P2_1/c$
a, Å	16.1742(14)	8.916(4)	8.4966(3)
b, Å	12.8053(10)	13.845(6)	15.9386(6)
c, Å	12.0272(10)	18.320(8)	15.7274(6)
β, °	111.574(2)	90.016(16)	90.3800(10)
cell volume, Å^3	2316.5(3)	2261.3(17)	2129.82(14)
Z	4	4	4
D_σ, g·cm^{-3}	1.853	1.840	1.960
μ, mm^{-1}	1.357	1.387	1.480
F(000)	1280	1248	1240
crystal size, mm	0.20 × 0.14 × 0.08	0.21 × 0.19 × 0.13	0.21 × 0.18 × 0.14
θ limits, °	2.089−26.999	1.844−25.0410	1.819−27.000
reflections collected	32,838	24,628	31,189
independent reflections	5017 [R_{int} = 0.0473]	4008 [R_{int} = 0.0585]	4638 [R_{int} = 0.0322]
data/restraints/parameters	50,176/106/322	4008/212/329	4638/0/292
goodness on fit on F^2	1.414	1.126	1.223
R_1 ($I > 2\sigma(I)$)	0.0589	0.0450	0.0253
wR_2 (all data)	0.1254	0.1059	0.0531
largest diff. peak and hole, e Å^{-3}	1.573/−1.078	1.050/−1.301	0.906/−0.551

■ ASSOCIATED CONTENT

Supporting Information

The Supporting Information is available free of charge at https://pubs.acs.org/doi/10.1021/acs.organomet.2c00060.

Synthetic procedures and the NMR spectra of products (PDF)

Accession Codes

CCDC 2128496−2128498 contain the supplementary crystallographic data for this paper. These data can be obtained free of charge via www.ccdc.cam.ac.uk/data_request/cif, or by emailing data_request@ccdc.cam.ac.uk, or by contacting The Cambridge Crystallographic Data Centre, 12 Union Road, Cambridge CB2 1EZ, UK; fax: +44 1223 336033.

■ AUTHOR INFORMATION

Corresponding Author

Fabio Marchetti − *Department of Chemistry and Industrial Chemistry, University of Pisa, Pisa I-56124, Italy;* orcid.org/0000-0002-3683-8708; Email: fabio.marchetti1974@unipi.it

Authors

Giulio Bresciani − *Department of Chemistry and Industrial Chemistry, University of Pisa, Pisa I-56124, Italy*

Stefano Zacchini − *Department of Industrial Chemistry "Toso Montanari", University of Bologna, Bologna I-40136, Italy;* orcid.org/0000-0003-0739-0518

Guido Pampaloni − *Department of Chemistry and Industrial Chemistry, University of Pisa, Pisa I-56124, Italy;* orcid.org/0000-0002-6375-4411

Complete contact information is available at: https://pubs.acs.org/10.1021/acs.organomet.2c00060

Notes

The authors declare no competing financial interest.

CCDC reference numbers 2128496 (**4**), 2128497 (**7**), and 2128498 (**8**) contain the supplementary crystallographic data for the X-ray studies reported in this work. These data are available free of charge at http://www.ccdc.cam.ac.uk/structures.

■ ACKNOWLEDGMENTS

We thank the University of Pisa for financial support (Fondi di Ateneo 2020).

■ REFERENCES

(1) ((a)) Thommes, K.; Strezov, V. *Fischer−Tropsch Synthesis from Biosyngas, in book Biomass Processing Technologies*, CRC press, 2014, pp. 309−356. ((b)) van de Loosdrecht, J.; Botes, F.G.; Ciobica, I.M.; Ferreira, A.; Gibson, P.; Moodley, D.J.; Saib, A.M.; Visagie, J.L.; Weststrate, C.J.; Niemantsverdriet, J. W. *Fischer−Tropsch Synthesis: Catalysts and Chemistry, Comprehensive Inorganic Chemistry II*; Elsevier Ed., 2013 p. 525-557. ((c)) *Greener Fischer-Tropsch Processes for Fuels and Feedstocks*. Edited by Maitlis, P. M.; de Klerk, A. Wiley Ed. 2013.

(2) (a) Chen, W.; Filot, I. A. W.; Pestman, R.; Hensen, E. J. M. Mechanism of Cobalt-Catalyzed CO Hydrogenation: 2. Fischer Tropsch Synthesis. *ACS Catal.* **2017**, *7*, 8061−8071. (b) Foppa, L.; Iannuzzi, M.; Coperet, C.; Comas-Vives, A. Facile Fischer-Tropsch Chain Growth from CH_2 Monomers Enabled by the Dynamic CO Adlayer. *ACS Catal.* **2019**, *9*, 6571−6582. ((c)) Maitlis, P. M. Mechanistic Studies Related to the Fischer-Tropsch Hydrocarbon Synthesis and Some Cognate Processes. In *Greener Fischer-Tropsch Processes for Fuels and Feedstocks*; Maitlis, P. M.; de Klerk, A. Wiley Ed.: Weinheim, 2013; pp. 237−265.

(3) (a) Jahangiri, H.; Bennett, J.; Mahjoubi, P.; Wilson, K.; Gu, S. A review of advanced catalyst development for Fischer-Tropsch synthesis of hydrocarbons from biomass derived syn-gas. *Catal. Sci. Technol.* **2014**, *4*, 2210−2229. (b) Chen, Y.; Wei, J.; Duyar, M. S.; Ordomsky, V. V.; Khodakov, A. Y.; Liu, J. Carbon-based catalysts for Fischer−Tropsch Synthesis. *Chem. Soc. Rev.* **2021**, *50*, 2337−2366.

(4) (a) Shetty, S. G.; Ciobıca, I. M.; Hensen, E. J. M.; van Santen, R. A. Site regeneration in the Fischer−Tropsch synthesis reaction: a synchronized CO dissociation and C−C coupling pathway. *Chem. Commun.* **2011**, *47*, 9822−9824. (b) Turner, M. L.; Marsih, N.; Mann, B. E.; Quyoum, R.; Long, H. C.; Maitlis, P. M. Investigations by ^{13}C NMR Spectroscopy of Ethene-Initiated Catalytic CO Hydrogenation. *J. Am. Chem. Soc.* **2002**, *124*, 10456−10472. (c) Teimouri, Z.; Abatzoglou, N.; Dalai, A. K. Kinetics and Selectivity Study of Fischer−Tropsch Synthesis to C_5+ Hydrocarbons: A Review. *Catalysts* **2021**, *11*, 330. (d) Han, Y.-S.; Hill, A. F.; Kong, R. Y. An unusual alkylidyne homologation. *Chem. Commun.* **2018**, *54*, 2292−2295.

(5) Turner, M. L.; Long, H. C.; Shenton, A.; Byers, P. K.; Maitlis, P. M. The Alkenyl Mechanism for Fischer-Tropsch Surface Methylene Polymerisation; the Reactions of Vinylic Probes with CO/H_2 over Rhodium Catalysts. *Chem. − Eur. J.* **1995**, *1*, 549−556.

(6) (a) Maitlis, P. M.; Zanotti, V. Organometallic Models for Metal Surface Reactions: Chain Growth Involving Electrophilic Methylidynes in the Fischer−Tropsch Reaction. *Catal. Lett.* **2008**, *122*, 80−83. (b) Bresciani, G.; Schoch, S.; Biancalana, L.; Zacchini, S.; Bortoluzzi, M.; Pampaloni, G.; Marchetti, F. Cyanide − alkene competition in a diiron complex and isolation of a multisite (cyano)alkylidene−alkene species. *Dalton Trans.* **2022**, *51*, 1936−1945.

(7) Casey, C. P.; Fagan, P. J.; Miles, W. H. Synthesis and Interconversions of Dinuclear Iron Complexes with .mu.-methyl, .mu.-methylene, and .mu.-methylidyne Ligands. *J. Am. Chem. Soc.* **1982**, *104*, 1134−1136.

(8) (a) Casey, C. P.; Austin, E. A. Photochemical Reactions of Diiron .mu.-Alkenylidene Complexes with Hydrogen, Trialkylsilanes, and Diazo Compounds: Cleavage to Alkenes, Vinylsilanes, and Allenes. *J. Am. Chem. Soc.* **1988**, *110*, 7106−7113. (b) Casey, C. P.; Austin, E. A.; Rheingold, A. L. Reaction of Diiron .mu.-Alkytidyne Complexes with Diazo Compounds. *Organometallics* **1987**, *6*, 2157−2164.

(9) (a) Akita, M.; Hua, R.; Knox, S. A. R.; Moro-oka, Y.; Nakanishi, S.; Yates, M. I. Specific alkylidene coupling of the labile diruthenium bridging methylene complex $[(\eta\text{-}C_5H_5)_2Ru_2Cp_2(\mu\text{-}CH_2)(CO)_2(MeCN)]$ with diazoalkanes (N_2=CR_2) giving alkenic products. *Chem. Commun.* **1997**, 51−52. (b) Dennett, J. N. L.; Knox, S. A. R.; Charmant, J. P. H.; Gillon, A. L.; Orpen, A. G. Synthesis and reactivity of μ-butadienyl diruthenium cations. *Inorg. Chim. Acta* **2003**, *354*, 29−40. (c) Colborn, R. E.; Davies, D. L.; Dyke, A. F.; Knox, S. A. R.; Mead, K. A.; Orpen, A. G.; Guerchais, J. E.; Roué, J. Organic Chemistry of Dinuclear Metal Centres. Part 12. Synthesis, X-Ray Crystal Structure, and Reactivity of the di-μ-alkylidene Complex $[Ru_2(CO)_2(\mu\text{-}CHMe)(\mu\text{-}CMe_2)(Cp)_2]$: Alkylidene Linking. *J. Chem. Soc., Dalton Trans.* **1989**, 1799−1805.

(10) (a) Bruce, G. C.; Knox, S. A. R.; Phillips, A. J. Synthesis of Butadiene via Vinyl-Ethylene Combination at a Diruthenium Centre. *J. Chem. Soc., Chem. Commun.* **1990**, 716−718. (b) Bruce, G. C.; Gangnus, B.; Garner, S. E.; Knox, S. A. R.; Orpen, A. G.; Phillips, A. J. Vinyl Homologation via Methyl Migration to μ-Vinyl at a Diruthenium Centre. *J. Chem. Soc., Chem. Commun.* **1990**, 1360−1362.

(11) Ohata, J.; Teramoto, A.; Fujita, H.; Takemoto, S.; Matsuzaka, H. Linear Hydrocarbon Chain Growth from a Molecular Diruthenium Carbide Platform. *J. Am. Chem. Soc.* **2021**, *143*, 16105−16112.

(12) (a) Hoel, E. L.; Ansell, G. B.; Leta, S. Thermal and Photochemical Rearrangements of a Bridging Cyclopropylidene Ligand to Allene In a Diiron Complex. *Organometallics* **1986**, *5*, 585−587. (b) Casey, C. P.; Austin, E. A. Photochemical reactions of diiron .mu.-alkenylidene complexes with hydrogen, trialkylsilanes, and diazo compounds: cleavage to alkenes, vinylsilanes and allenes. *J. Am. Chem. Soc.* **1988**, *110*, 7106−7113.

(13) Doherty, N. M.; Elschenbroich, C.; Kneuper, H. J.; Knox, S. A. R. 'Side-on' co-ordination of vinylidene at a dimolybdenum centre. *J. Chem. Soc., Chem. Commun.* **1985**, *3*, 170−171.

(14) Fildes, M. J.; Knox, S. A. R.; Orpen, A. G.; Turner, M. L.; Yates, M. I. Synthesis of trimethylenemethane by combination of methylene with allene at a diruthenium centre: X-ray structure of $[Ru_2(CO)(\mu\text{-}CO)\{\mu\text{-}\eta^1,\eta^3\text{-}CH_2C(CH_2)_2\}(\eta\text{-}C_5H_5)_2]$. *J. Chem. Soc., Chem. Commun.* **1989**, *21*, 1680−1682.

(15) Torkelson, J. R.; McDonald, R.; Cowie, M. Binuclear Complexes as Models for Adjacent-Metal Involvement in C-H Bond-Cleavage and C-C Bond-Formation Steps Relevant to Fischer-Tropsch Chemistry. *J. Am. Chem. Soc.* **1998**, *120*, 4047−4048.

(16) A variety of other coordination modes for allenyl ligands has been reported, see for instance: (a) Shi, X.; Li, S.; Reiß, M.; Spannenberg, A.; Holtrichter-Roßmann, T.; Reiß, F.; Beweries, T. 1-Zirconacyclobuta-2,3-dienes: synthesis of organometallic analogs of elusive 1,2- cyclobutadiene, unprecedented intramolecular C−H activation, and reactivity studies. *Chem. Sci.* **2021**, *12*, 16074−16084. (b) Saito, M.; Kojima, S.; Inagaki, A.; Seki, K.; Takao, T. Effect of ring size on the properties of μ3-Cycloalkyne complexes: Synthesis of triruthenium complexes containing a perpendicularly coordinated μ3-Allenyl ligand. *J. Organomet. Chem.* **2019**, *885*, 7−20. (c) Wojcicki, A. Trimethylenemethane, oxatrimethylenemethane, and azatrimethylenemethane complexes of platinum from epropargyl/allenyl precursors. *New J. Chem.* **1997**, *21*, 733−737. (d) Hughes, R. P.; Larichev, R. B.; Zakharov, L. N.; Rheingold, A. L. Carbon-fluorine bond activation coupled with alkynyl migration to give fluorinated allenyl complexes of iridium. *Organometallics* **2006**, *25*, 3943−3947.

(17) (a) Doherty, S.; Elsegood, M. R. J.; Clegg, W.; Scanlan, T. H.; Rees, N. H. An unprecedented regiospecific attack of phosphorus nucleophiles at C_α, of the allenyl ligand in $[Fe_2(CO)_6(\mu\text{-}PPh_2)\{\mu\text{-}\eta^1{:}\eta^2_{\alpha,\beta}\text{-}(H)C_\alpha{=}C_\beta{=}C_\gamma H_2\}]$. *Chem. Commun.* **1996**, 1545−1546. (b) Doherty, S.; Elsegood, M. R. J.; Clegg, W.; Waugh, M. Competitive Nucleophilic Attack at CO and Cβ of the Allenyl Group in $[Fe_2(CO)_6(\mu\text{-}PPh_2)(\mu\text{-}\eta^1{:}\eta^2\text{-}(H)C_\alpha{=}C_\beta{=}C_\gamma H_2)]$. X-ray Crystal Structures of $[Fe_2(CO)_5(\mu\text{-}PPh_2)(\mu\text{-}\eta^1(O){:}\eta^1(C){:}\eta^2(C)\text{-}\{O{=}C(N^tBuH)CH_2\}C{=}CH_2)]\cdot 0.5C_6H_{14}$ and $[Fe_2(CO)_6(\mu\text{-}PPh_2)(\mu\text{-}\eta^1{:}\eta^1\text{-}CH_2C(NCyH)CH_2)]\cdot$MeCN. *Organometallics* **1996**, *15*, 2688−2691. (c) Blenkiron, P.; Corrigan, J. F.; Taylor, N. J.; Carty, A. J.; Doherty, S.; Elsegood, M. R. J.; Clegg, W. New Reaction Pathways for $\mu\text{-}\eta^1,\eta^2$-Allenyl Ligands: On-Off Allenyl Coordination and CO Insertion into the Hydrocarbyl Bridge in $Ru_2(CO)_6(\mu\text{-}PPh_2)\{\mu\text{-}\eta^1{:}\eta^2_{\alpha,\beta}\text{-}C(Ph){=}C{=}CPh_2\}$. *Organometallics* **1997**, *16*, 297−300. (d) Doherty, S.; Hogarth, G.; Waugh, M.; Clegg, W.; Elsegood, M. R. J. Conversion of σ,η-Allenyl Group into a σ,σ-(Diphenylphosphino)allyl and a Hexa-1,3,5-triene-2,6-diyl Ligand at a Diiron Center. *Organometallics* **2000**, *19*, 5696−5708. (e) Boni, A.; Funaioli, T.; Marchetti, F.; Pampaloni, G.; Pinzino, C.; Zacchini, S. Electrochemical, EPR and computational results on $[Fe_2Cp_2(CO)_2]$-based complexes with a bridging hydrocarbyl ligand. *J. Organomet. Chem.* **2011**, *696*, 3551−3556.

(18) Boni, A.; Marchetti, F.; Pampaloni, G.; Zacchini, S. Cationic Diiron and Diruthenium μ-Allenyl Complexes: Synthesis, X-Ray Structures and Cyclization Reactions with Ethyldiazoacetate/Amine Affording Unprecedented Butenolide- and Furaniminium-Substituted Bridging Carbene Ligands. *Dalton Trans.* **2010**, *39*, 10866−10875.

(19) Knox, S. A. R.; Marchetti, F. Additions and intramolecular migrations of nucleophiles in cationic diruthenium μ-allenyl complexes. *J. Organomet. Chem.* **2007**, *692*, 4119−4128.

(20) Dyke, A. F.; Knox, S. A. R.; Naish, P. J.; Taylor, G. E. Organic chemistry of dinuclear metal centres. Part 1. Combination of alkynes with carbon monoxide at di-iron and diruthenium centres: crystal structure of $[Ru_2(CO)(\mu\text{-}CO)\{\mu\text{-}\sigma{:}\eta^3\text{-}C(O)C_2Ph_2\}(\eta\text{-}C_5H_5)_2]$. *J. Chem. Soc., Dalton Trans.* **1982**, 1297−1307.

(21) Luh, T.-Y. Trimethylamine N-Oxide-A Versatile Reagent For Organometallic Chemistry. *Coord. Chem. Rev.* **1984**, *60*, 255−276.

(22) (a) Straub, T.; Haukka, M.; Pakkanen, T. A. Unbridged homo and hetero dinuclear complexes of Group 6 and 8 metals: synthesis, characterization and comparison of X-ray crystallographic data. *J. Organomet. Chem.* **2000**, *612*, 106−116. (b) Uehara, K.; Hikichi, S.; Inagaki, A.; Akita, M. Xenophilic Complexes Bearing a TpR Ligand: The Two Metal Centers are Held Together not by Covalent Interaction but by Electrostatic Attraction. *Chem. − Eur. J.* **2005**, *11*, 2788−2809.

(23) (a) Forrow, N. J.; Knox, S. A. R.; Morris, M. J.; Orpen, A. G. Synthesis, X-ray structure, and reactivity of $[Ru_3H_3(CO)_3(\eta\text{-}C_5H_5)_3]$: an entry into the organic chemistry of the triruthenium centre. *J. Chem. Soc., Chem. Commun.* **1983**, 234−235. (b) King, P. J.; Knox, S. A. R.; McCormick, G. J.; Orpen, A. G. Synthesis and reactivity of dimetallacyclopentenone complexes $[Ru_2(CO)(\mu\text{-}CO)\{\mu\text{-}C(O)\text{-}CR^1CR^2\}(\eta\text{-}C_5H_5)_2]$ (R^1 = Me or Ph; R^2 = CO_2Me). *J. Chem. Soc., Dalton Trans.* **2000**, 2975−2982. (c) Nataro, C.; Thomas, L. M.; Angelici, R. J. Cyclopentadienyl Ligand Effects on Enthalpies of Protonation of the Ru−Ru Bond in $Cp'_2Ru_2(CO)_4$ Complexes. *Inorg. Chem.* **1997**, *36*, 6000−6008. (d) Cesari, C.; Bortoluzzi, M.; Femoni, C.; Iapalucci, M. C.; Zacchini, S. One-pot atmospheric pressure synthesis of $[H_3Ru_4(CO)_{12}]^-$. *Dalton Trans.* **2021**, *50*, 9610−9622.

(24) Cordero, B.; Gómez, V.; Platero-Prats, A.; Revés, M.; Echeverría, J.; Cremades, E.; Barragán, F.; Alvarez, S. Covalent radii revisited. *Dalton Trans.* **2008**, 2832−2838.

(25) (a) Hazari, N.; Hruszkewycz, D. P. Dinuclear PdI complexes with bridging allyl and related ligands. *Chem. Soc. Rev.* **2016**, *45*, 2871−2899. (b) Cabeza, J. A.; del Rio, I.; Fernandez-Colinas, J. M.; Perez-Carreno, E.; Vazquez-Garcia, D. From Allenes to Edge-Bridging Allyl Ligands or Face-Capping Alkenyl Ligands on a Triruthenium Hydrido Carbonyl Cluster: An Experimental and DFT Computational Study. *Organometallics* **2010**, *29*, 4818−4828.

(26) (a) Hossain, M. I.; Ghosh, S.; Hogarth, G.; Golzar Hossain, G. M.; Kabir, S. E. Bridging allyl ligands upon allene insertion into electron-deficient triosmium-hydride clusters $[Os_3(CO)_9(\mu_3\text{-}NSC_7H_3R)(\mu\text{-}H)]$ (R = H, Me). *J. Organomet. Chem.* **2011**, *696*, 3036−3039. (b) MacDougall, T. J.; Ferguson, M. J.; McDonald, R.; Cowie, M. Diverse Coordination Modes and Transformations of Allenes at Adjacent Iridium/Osmium Centers. *Organometallics* **2012**, *31*, 4516−4528.

(27) Mazzoni, R.; Salmi, M.; Zanotti, V. C-C Bond Formation in Diiron Complexes. *Chem. − Eur. J.* **2012**, *18*, 10174−10194.

(28) (a) Doherty, N. M.; Howard, J. A. K.; Knox, S. A. R.; Terrill, N. J.; Yates, M. I. Reactivity of Alkenes at a Diruthenium Centre: Combination with Methylene and Oxidative Activation. *J. Chem. Soc., Chem. Commun.* **1989**, 638−640. (b) Busetto, L.; Salmi, M.; Zacchini, S.; Zanotti, V. Olefin−aminocarbyne coupling in diiron complexes: Synthesis of new bridging aminoallylidene complexes. *J. Organomet. Chem.* **2008**, *693*, 57−67.

(29) (a) Ciancaleoni, G.; Zacchini, S.; Zanotti, V.; Marchetti, F. DFT Mechanistic Insights into the Alkyne Insertion Reaction Affording Diiron μ-Vinyliminium Complexes and New Functionalization Pathways. *Organometallics* **2018**, *37*, 3718−3731. (b) Marchetti, F.; Zacchini, S.; Zanotti, V. Photochemical Alkyne Insertions into the Iron-Thiocarbonyl Bond of $[Fe_2(CS)(CO)_3(Cp)_2]$. *Organometallics* **2016**, *35*, 2630−2637. (c) Dennett, J. N. L.; Knox, S. A. R.; Anderson, K. M.; Charmant, J. P. H.; Guy Orpen, A. The synthesis of $[FeRu(CO)_2(\mu\text{-}CO)_2(Cp)(Cp^*)]$ and convenient entries to its organometallic chemistry. *Dalton Trans.* **2005**, 63−73. (d) Casey, C. P.; Ha, Y.; Powell, D. R. Synthesis and Reactions of Dirhenium Alkenylidene and Alkylidyne Complexes. *J. Am. Chem. Soc.* **1994**, *116*, 3424−3428.

(30) The alkenylation of a range of monosubstituted allenes was recently achieved at one terminal carbon via C-H activation by Pd catalyst: Schreib, B. S.; Son, M.; Aouane, F. A.; Baik, M.-H.; Carreira, E. M. Allene $C(sp^2)$−H Activation and Alkenylation Catalyzed by Palladium. *J. Am. Chem. Soc.* **2021**, *143*, 21705−21712.

(31) (a) Howell, J. A. S.; Rowan, A. J. Synthesis and fluxional character of complexes of the type $[M_2(Cp)_2(CO)_3(CNR)]$ (M = Fe or Ru, cp = η-C_5H_5). *J. Chem. Soc., Dalton Trans.* **1980**, *3*, 503−510. (b) Biancalana, L.; Marchetti, F. Aminocarbyne ligands in organometallic chemistry. *Coord. Chem. Rev.* **2021**, *449*, 214203.

(32) Menges, F. *Spectragryph - optical spectroscopy software*, Version 1.2.5, @ 2016−2017, http://www.effemm2.de/spectragryph.

(33) Bresciani, G.; Marchetti, F.; Pampaloni, G. Carboxylation of terminal alkynes promoted by silver carbamate at ambient pressure. *New J. Chem.* **2019**, *43*, 10821−10825.

(34) Fulmer, G. R.; Miller, A. J. M.; Sherden, N. H.; Gottlieb, H. E.; Nudelman, A.; Stoltz, B. M.; Bercaw, J. E.; Goldberg, K. I. NMR Chemical Shifts of Trace Impurities: Common Laboratory Solvents, Organics, and Gases in Deuterated Solvents Relevant to the Organometallic Chemist. *Organometallics* **2010**, *29*, 2176−2179.

(35) Willker, W.; Leibfritz, D.; Kerssebaum, R.; Bermel, W. Gradient selection in inverse heteronuclear correlation spectroscopy. *Magn. Reson. Chem.* **1993**, *31*, 287−292.

(36) Sheldrick, G. M. Crystal structure refinement with SHELXL. *Acta Crystallogr. C* **2015**, *71*, 3−8.

(37) Flack, H. D. On enantiomorph-polarity estimation. *Acta Crystallogr. A* **1983**, *39*, 876−881.

https://doi.org/10.1021/acs.organomet.2c00060
Organometallics 2022, 41, 1006−1014